ORIGINAL RESEARCH

Hyperglycemia Suppresses Calcium Phosphate–Induced Aneurysm Formation Through Inhibition of Macrophage Activation

Teruyoshi Tanaka, PhD; Yuichiro Takei, PhD;* Dai Yamanouchi, MD, PhD

***Background*—**The aim of this study was to elucidate aspects of diabetes mellitus–induced suppression of aneurysm. We hypothesized that high glucose suppresses aneurysm by inhibiting macrophage activation via activation of Nr1h2 (also known as liver X receptor β), recently characterized as a glucose-sensing nuclear receptor.

***Methods and Results*—**Calcium phosphate ($CaPO_4$)–induced aneurysm formation was significantly suppressed in the arterial wall in type 1 and 2 diabetic mice. A murine macrophage cell line, RAW264.7, was treated with tumor necrosis factor α (TNF-α) plus $CaPO_4$ and showed a significant increase in matrix metalloproteinase 9 (Mmp9) mRNA and secreted protein expression compared with TNF-α alone. Elevated Mmp9 expression was significantly suppressed by hyperglycemic conditions (15.5 mmol/L glucose) compared with normoglycemic conditions (5.5 mmol/L glucose) or normoglycemic conditions with high osmotic pressure (5.5 mmol/L glucose +10.0 mmol/L mannitol). Nr1h2 mRNA and protein expression were suppressed by treatment with TNF-α plus $CaPO_4$ but were restored by hyperglycemic conditions. Activation of Nr1h2 by the antagonist GW3965 during stimulation with TNF-α plus $CaPO_4$ mimicked hyperglycemic conditions and inhibited Mmp9 upregulation, whereas the deactivation of Nr1h2 by small interfering RNA (siRNA) under hyperglycemic conditions canceled the suppressive effect and restored Mmp9 expression induced by TNF-α plus $CaPO_4$. Moreover, Nr1h2 activation with GW3965 significantly suppressed $CaPO_4$-induced aneurysm in mice compared with vehicle-injected control mice.

***Conclusions*—**Our results show that hyperglycemia suppresses macrophage activation and aneurysmal degeneration through the activation of Nr1h2. Although further validation of the underlying pathway is necessary, targeting Nr1h2 is a potential therapeutic approach to treating aneurysm. **(*J Am Heart Assoc*. 2016;5:e003062 doi: 10.1161/JAHA.115.003062)**

Key Words: aneurysm • diabetes mellitus • LXRβ • macrophage activation • metalloproteinases • Nr1h2

Aortic aneurysm is a significant medical condition with high prevalence in men aged >65 years and significant mortality.[1] Previous studies suggested that the pathogenesis of aneurysm is closely associated with chronic inflammation of the aortic wall, the local activation of proteinases, and the degradation of matrix proteins by matrix metalloproteinases produced from activated macrophages.[1,2] Currently, surgical intervention with either open repair or endovascular stent graft placement is the only proven treatment for aneurysm, but it has significant associated morbidity and mortality, indicating the urgent need for alternative therapeutic strategies.

Diabetes mellitus (DM) is also a significant medical condition. A major feature of DM-induced vascular pathology is severe calcification of the medial layer of the artery that eventually causes stenosis or occlusion and ischemic changes to the target organs in conditions such as coronary artery disease, peripheral artery disease, and ischemic stroke.[3,4] It is interesting that recent large epidemiological studies have shown that DM is an independent negative risk factor for aneurysm, although it shares most of the same common risk factors as stenotic arterial disease, including male sex, aging, hypertension, dyslipidemia, and smoking.[5,6]

Nr1h1 and Nr1h2 (also known as liver X receptor [LXR] α and β, respectively) were recently characterized as glucose-sensing nuclear receptors, although they have been identified for some time.[7] There has also been great interest in these

From the Division of Vascular Surgery, Department of Surgery, Wisconsin Institute for Medical Research, University of Wisconsin School of Medicine and Public Health, Madison, WI.

Accompanying Figures S1 and S2 are available at http://jaha.ahajournals.org/content/5/3/e003062/suppl/DC1

*Dr Yuichiro Takei is currently located at the Department of Calcified Tissue Biology, Hiroshima University Institute of Biomedical & Health Sciences, 1-2-3 Kasumi Minami-ku, Hiroshima 734-8553, Japan.

Correspondence to: Dai Yamanouchi, MD, PhD, Division of Vascular Surgery, Department of Surgery, Wisconsin Institute for Medical Research, University of Wisconsin School of Medicine and Public Health, 1111 Highland Ave. 5148, Madison, WI 53705. E-mail: yamano@surgery.wisc.edu

Received December 8, 2015; accepted February 17, 2016.

receptors as novel therapeutic targets for inflammatory diseases because they inhibit inflammatory gene expression downstream of signaling mediated by Toll-like receptor 4, interleukin 1b, and tumor necrosis factor α (TNF-α).[8,9] Robertson Remen et al[10] demonstrated the effect of the Nr1h (LXR) agonist GW3965 in lipopolysaccharide-induced differentiation of bone marrow–derived macrophages into osteoclasts via an Nr1h2-dependent (but not an Nr1h1-dependent) mechanism.

Although there have been several reports regarding the underlying mechanisms of DM suppression of aneurysm, the effects of DM on macrophages and aneurysmal degeneration are still controversial. Macrophage subpopulations identified by CD68, a macrophage marker, were reported to be significantly higher in diabetic versus nondiabetic patients.[11] In contrast, Miyama et al[12] showed that hyperglycemia attenuates macrophage infiltration in a mouse model of aneurysm induced by porcine pancreatic elastase. In this study, we focused on how high glucose affects macrophage activation and aneurysm formation through Nr1h2.

Materials and Methods

Materials

TNF-α and GW3965 were purchased from Peprotech and Santa Cruz Biotechnology. Streptozotocin (STZ) was purchased from Sigma-Aldrich. All chemicals used in this study were of the highest purity available.

Cell Culture

Murine monocytic RAW264.7 cells were purchased from American Type Culture Collection (Manassas, VA) and maintained in Dulbecco's modified Eagle's medium (Mediatech) containing 10% FBS (Mediatech), 100 IU/mL penicillin, and 100 μg/mL streptomycin (Mediatech). For macrophage activation, 5×10^5 cells were plated per well in a 6-well plate and maintained in minimal essential medium α (Mediatech) supplemented with 10% charcoal-stripped FBS with antibiotics.

Cell Viability

RAW264.7 cells were cultivated in 96-well plates (4000 cells per well) 1 day before treatment and were cultured with or without TNF-α plus calcium phosphate ($CaPO_4$), mannitol, and high glucose. The cells were combined with MTT solution (50 ng per well) and incubated for 4 hours. Acid isopropanol (0.04 N HCl in isopropanol) and 3% sodium lauryl sulfate were added to dissolve the reduced MTT crystals (formazan) present in the cells. After mixing, the absorbance was measured at 595 nm, with 655 nm as the reference, using a microplate reader.

Mouse Model of Aneurysm and Treatment

C57BL/6 or KK.Cg-Ay/J mice aged 10 weeks were obtained from the Jackson Laboratory (Bar Harbor, ME). The procedures for creating our modified $CaCl_2$-induced mouse model of aneurysm were described previously.[13] We applied the procedure for the infrarenal aorta to the carotid artery in this study. Briefly, 0.5 mol/L $CaCl_2$-soaked gauze was applied perivascularly for 10 minutes to the carotid artery. The gauze was replaced with PBS-soaked gauze for 5 minutes, and the incised area was sutured. The excess $CaCl_2$ is converted into $CaPO_4$, and the crystals act as adjuvants. After 1 to 4 weeks, the mice were sacrificed, and the carotid arteries were collected after fixing by perfusion with 4% paraformaldehyde. The diameter of the artery at the time of the initial surgery and sacrifice was measured with an electronic digital caliper (VWR International). All animal procedures were conducted in accordance with experimental protocols that were approved by the institutional animal care and use committee at the University of Wisconsin, Madison (protocol M02394).

siRNA Transfection

RAW264.7 cells were transfected with either predesigned Nr1h2 siRNA (Invitrogen) or Silencer Negative Control #1 siRNA (Invitrogen) using Lipofectamine RNAiMAX transfection reagent (Invitrogen), according to the manufacturer's recommendations. Transfected cells (5×10^5) were seeded in 6-well plates for mRNA extraction.

Histological and Immunohistochemical Analysis

The murine carotid artery tissues obtained were fixed with 4% paraformaldehyde overnight. The samples were then embedded with OCT compound (Sakura Tissue Tek), frozen, and sectioned at a thickness of 6 μm per section. For histological analysis, the sections were stained with hematoxylin and eosin and observed by light microscopy (Olympus BH-2). Immunofluorescent staining was performed with rat anti-MOMA-2 (ab33451; Abcam) and donkey anti–rat Alexa 488 (Molecular Probes, Invitrogen). TO-PRO-3 stain (Molecular Probes, Invitrogen) was used to identify nuclei. Fluorescent staining was visualized, and digital images were taken on a Nikon A1R Laser Scanning Confocal imaging system with the appropriate argon-beam lasers.

Western Blotting

Protein extraction was performed at 0 to 4°C. Protein from cultured cells and isolated carotid arteries was extracted with a radioimmunoprecipitation assay buffer supplemented with a protease inhibitor cocktail (Cell Signaling Technology). Next,

20-μg samples were separated on 8%, 10%, or 12% polyacrylamide gels in Laemmli sample buffer and transferred electrophoretically onto polyvinylidene difluoride membranes. The membranes were blocked for 1 hour at room temperature in Tris-buffered saline containing 3% skim milk powder. The primary antibodies used for Western blotting included rabbit matrix metalloproteinase 9 (Mmp9; ab38898; Abcam), rabbit Nr1h2 (sc-1001; Santa Cruz Biotechnology), and mouse α-tubulin (sc-23948; Santa Cruz Biotechnology) antibodies. Primary antibodies were detected using a horseradish peroxidase–conjugated secondary antibody and visualized with the enhanced chemiluminescence kit (Thermo Scientific) or SuperSignal West Femto Maximum Sensitivity Substrate (Thermo Scientific).

Quantitative Polymerase Chain Reaction

Total RNA was extracted from RAW264.7 cells using an RNeasy Plus Mini kit (Qiagen), according to the manufacturer's instructions. Quantitative polymerase chain reaction was performed with SYBR Green dye in a 7500 Fast Real-Time PCR System (ABI). Mouse *Gapdh* primers for quantitative polymerase chain reaction were purchased from Qiagen (PPM02946E). The sequences of other primers are as follows: *Mmp9*, F, 5′-CATTCGCGTGGATAAGGAGT-3′, and R, 5′-GTTCACCTCATGGTCCACCT-3′; *Nr1h2*, F, 5′-CAGCAGCTCAGGCCGGCAG-3′, and R, 5′-GGCTAGCTCGGTGAAGTGGG-3′. The expression level for each gene was normalized to the *Gapdh* expression level in the same sample.

Gelatin Zymography

Gelatin zymography was performed using cell culture medium. The medium was separated with 12.5% SDS-PAGE with 1 mg/mL gelatin incorporated into the gel mixture. Following electrophoresis at 4°C, the gel was washed in 2.5% Triton X-100 and incubated at 37°C for 16 hours in 50 mmol/L Tris-HCl (pH 7.4) containing 10 mmol/L $CaCl_2$ and 0.05% Brij 35. The gels were then stained with 0.5% Coomassie blue in 30% isopropanol and 10% acetic acid for 1 hour and destained in 12.5% isopropanol and 10% acetic acid.

Statistical Analysis

Data are reported as mean±SD. Statistical analysis was performed with GraphPad Prism version 4.00 (GraphPad Software, Inc). Comparisons between groups at a single time point were performed using the Student *t* test. Multiple comparisons among treatments were performed by 1-way ANOVA, followed by the Tukey range test. For testing 2 samples from the same population (Figures 1A, 1B, 2A, 2B, and 4E), the Wilcoxon rank sum test was used. *P* values <0.05 were accepted as statistically significant.

Results

Inhibition of $CaPO_4$-Induced Aneurysm Formation by Hyperglycemia in a Mouse Model of STZ-Induced Type 1 Diabetes

To examine the effect of hyperglycemia on aneurysm formation in type 1 DM, mice were intraperitoneally injected with STZ or control vehicle. After 7 days, aneurysm was induced with $CaPO_4$ in a surgical procedure. First, we measured body weight and blood glucose levels and confirmed successful induction of DM in the STZ-induced mice (Figure 1A and 1B). We then induced aneurysm and compared the maximum diameter of the artery after 4 weeks. As shown in Figure 1C and 1D, injection of STZ significantly suppressed aneurysm formation, based on the fold increase of the maximum diameter of the artery at the time of the initial surgery and sacrifice (1.8±0.2 versus 1.5±0.2, $P<0.05$) (Figure 1D). These results suggest that $CaPO_4$-induced aneurysm is suppressed by STZ-induced type 1 diabetes. Next, we examined whether macrophage accumulation was suppressed by STZ-induced DM in mice. Monocytes and macrophages, marked by MOMA-2, were localized mostly in the adventitia of mice in the $CaPO_4$-induced aneurysmal model (Figure 1E). The number of monocytes and macrophages was markedly decreased in STZ-induced mice compared with controls.

Inhibition of $CaPO_4$-Induced Aneurysm Formation by Hyperglycemia in a Mouse Model of KK-Ay Type 2 Diabetes

We examined the effect of type 2 DM on aneurysm formation by using KK-Ay mice, a model of type 2 DM. We first measured blood glucose levels and body weight. Although body weight showed no significant change in the 2 groups (Figure 2A), blood glucose levels were consistently higher in the KK-Ay mice than in the control mice (Figure 2B). We then induced aneurysm with $CaPO_4$ in both KK-Ay and control wild-type mice. As shown in Figure 2C, aneurysm formation was suppressed in KK-Ay mice compared with control mice. The diameter of the artery (fold increase) in the KK-Ay mice was significantly lower than in the control mice (1.8±0.2 versus 1.6±0.1, $P<0.05$) (Figure 2D). The numbers of monocytes and macrophages were also decreased in KK-Ay mice compared with controls (Figure 2E). These results suggest that $CaPO_4$-induced aneurysm formation was suppressed by the presence of type 2 diabetes in KK-Ay mice.

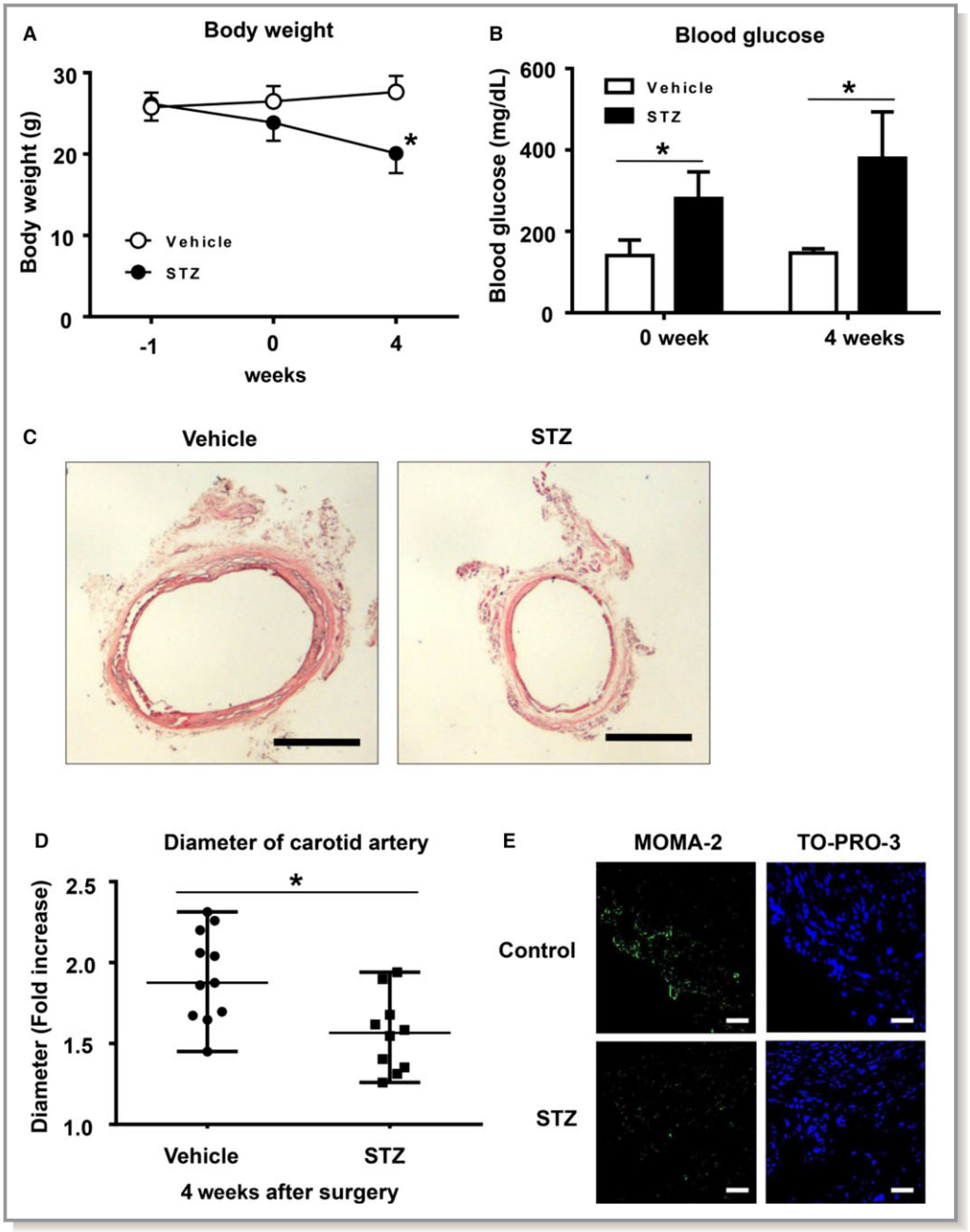

Figure 1. Hyperglycemia suppresses $CaPO_4$-induced aneurysm formation in a mouse model of type 1 diabetes. Male C57BL mice aged 12 weeks were intraperitoneally injected with 150 mg/mL STZ (n=10) or control vehicle (n=11). After 7 days, aneurysm was induced with $CaPO_4$ in a surgical procedure. Body weight (A) and blood glucose levels (B) were monitored. C, Representative images of carotid arteries stained with hematoxylin and eosin in control and type 1 diabetes model mice. Scale bar, 400 μm. D, The fold increase of carotid artery diameter at 4 weeks after surgery. E, Representative immunohistochemical images for MOMA-2 and TO-PRO-3 in carotid arteries. Scale bar, 30 μm. Values are presented as mean±SD; *P<0.05. $CaPO_4$ indicates calcium phosphate; STZ, streptozotocin.

Inhibition of TNF-α and $CaPO_4$-Induced Macrophage Activation by High-Glucose Treatment

TNF-α is known to be a key inflammatory mediator of aneurysm formation and macrophage activation.[14–16] We also reported that $CaPO_4$ crystals, a major component of arterial calcification, play an important role in aneurysm degeneration by inducing apoptosis of smooth muscle cells and macrophage infiltration.[13] Consequently, we established an in vitro aneurysm model by stimulating macrophages with TNF-α plus $CaPO_4$ crystals and used Mmp9 as a marker of classical

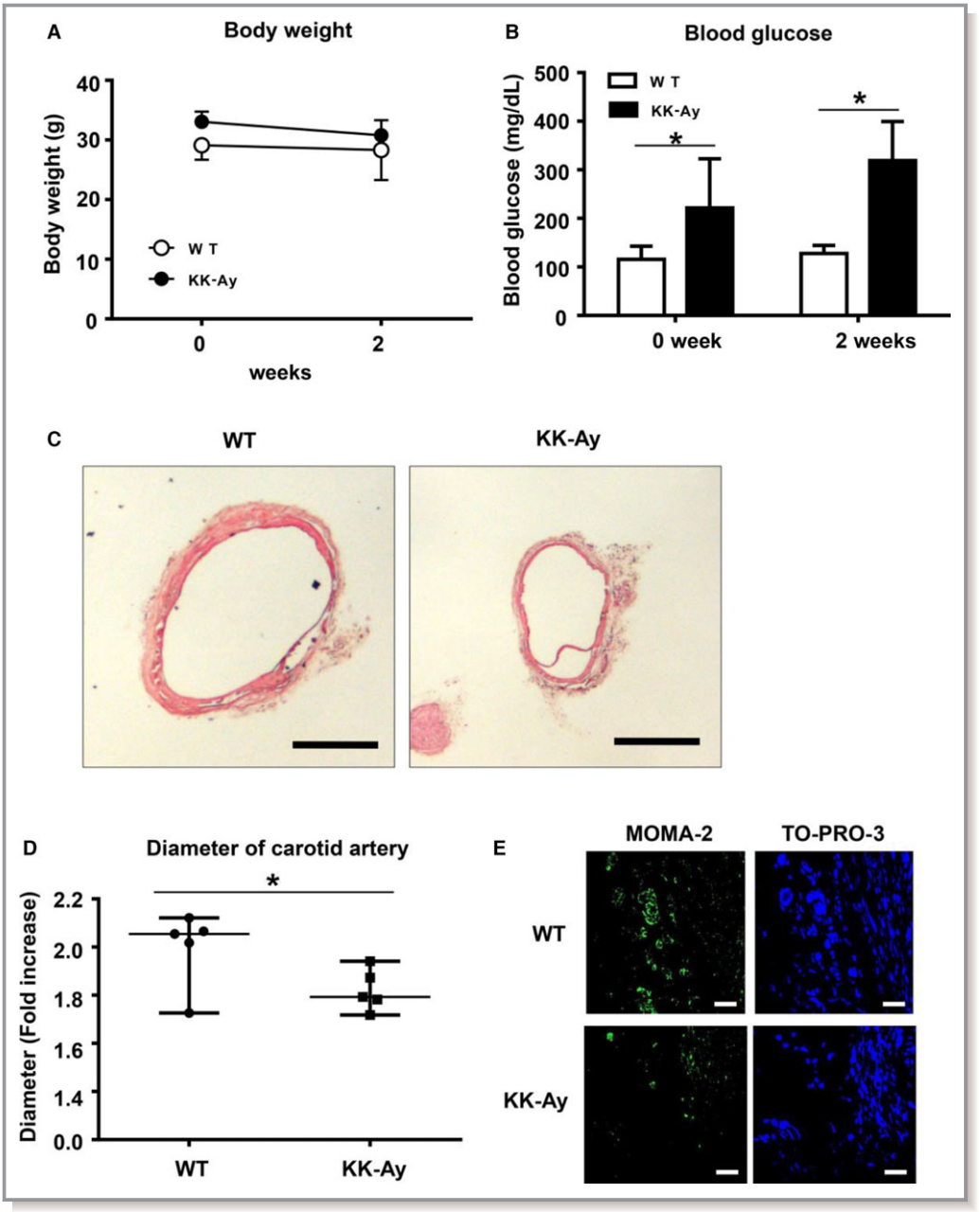

Figure 2. Hyperglycemia suppresses $CaPO_4$-induced aneurysm formation in a mouse model of type 1 diabetes. Male C57BL WT mice (n=5) or KK.Cg-Ay/J type 2 diabetes model mice (n=5) aged 12 weeks were used. Aneurysm was induced with $CaPO_4$ in a surgical procedure. Body weight (A) and blood glucose levels (B) were monitored. C, Representative images of carotid arteries stained with hematoxylin and eosin in WT and type 2 diabetes model mice. Scale bar, 400 μm. D, The fold increase of the carotid artery diameter 4 weeks after surgery. E, Representative immunohistochemical images for MOMA-2 and TO-PRO-3 in carotid arteries. Scale bar, 30 μm. Values are presented as mean±SD; *P<0.05. $CaPO_4$ indicates calcium phosphate; KK-Ay, KK.Cg-Ay/J; WT, wild type.

macrophage activation.[17,18] As shown in Figure 3A and 3B, treatment with TNF-α plus $CaPO_4$ significantly increased Mmp9 mRNA and secreted protein expression compared with TNF-α treatment alone (50.3±3.5 versus 21.0±1.0 and 7.5±1.7 versus 2.7±0.8, respectively, P<0.01), whereas $CaPO_4$ treatment alone did not affect Mmp9 expression. Next, RAW264.7 macrophages were treated with hyperglycemic conditions using 15.5 mmol/L glucose (corresponding to 279.2 mg/dL) to mimic DM-induced hyperglycemia. As shown in Figure 3C and 3D, high-glucose treatment significantly attenuated the elevated Mmp9 mRNA and secreted protein expression induced by TNF-α plus $CaPO_4$ (17.9±2.5

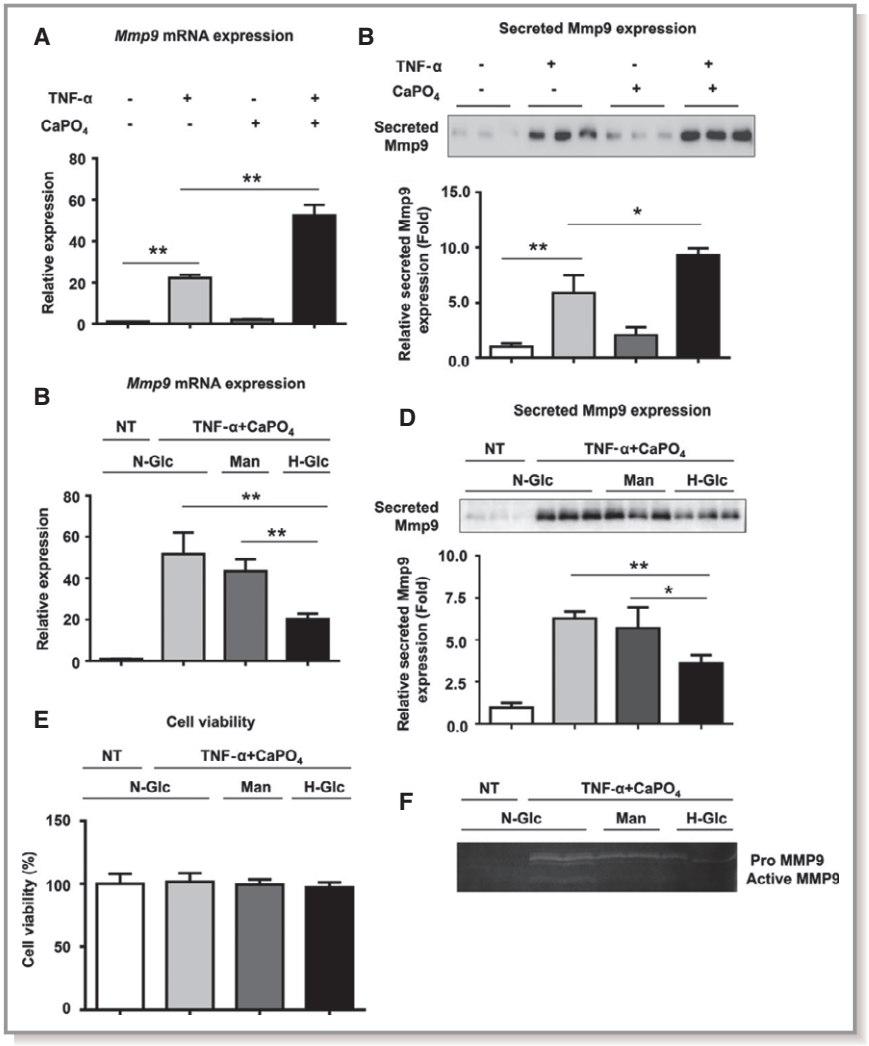

Figure 3. High-glucose treatment suppresses macrophage activation induced by TNF-α plus $CaPO_4$. A, Mmp9 mRNA expression levels in RAW264.7 cells after stimulation are shown relative to Gapdh expression. RAW264.7 cells were cultured with TNF-α and/or $CaPO_4$ for 2 days, and mRNA expression in the cell lysates was determined by quantitative polymerase chain reaction. B, Representative Western blot and densitometoric analysis of Mmp9 secreted protein expression levels in culture media from RAW264.7 cells treated with TNF-α and/or $CaPO_4$. The cells were treated with TNF-α and/or $CaPO_4$ for 5 days, and the culture medium was then analyzed. C, Mmp9 mRNA expression levels in RAW264.7 cells after stimulation are shown relative to Gapdh expression. RAW264.7 cells were cultured for 3 days under N-Glc (5.5 mmol/L glucose) without TNF-α plus $CaPO_4$ (NT control), N-Glc with TNF-α plus $CaPO_4$, Man (5.5 mmol/L glucose and 10.5 mmol/L mannitol) and TNF-α plus $CaPO_4$, and H-Glc (15.5 mmol/L glucose) with TNF-α plus $CaPO_4$. D, Representative Western blot and densitometoric analysis of secreted Mmp9 expression levels in culture media from RAW264.7 cells treated with TNF-α and/or $CaPO_4$. The cells were treated with NT or TNF-α plus $CaPO_4$ and N-Glc, Man, or H-Glc for 5 days, and then the culture medium was analyzed. E, Effect of high-glucose treatment on cell viability. The cells were treated with NT or TNF-α plus $CaPO_4$ and N-Glc, Man, or H-Glc for 2 days, and then the MTT assay was performed. F, MMP9 gelatinolytic activity according to gelatin zymography. The cells were treated with NT or TNF-α plus $CaPO_4$ under N-Glc, Man, or H-Glc for 5 days, and then the culture medium was analyzed. Values are presented as mean±SD for at least 3 replicates; $*P<0.05$. $**P<0.01$. Relative expression levels for Western blotting were quantified using the ImageJ program (National Institutes of Health). $CaPO_4$ indicates calcium phosphate; H-Glc, hyperglycemic conditions; Man, normoglycemic conditions with high osmotic pressure; Mmp9, matrix metalloproteinase 9; N-Glc, normoglycemic conditions; NT, no treatment; qPCR, quantitative polymerase chain reaction; TNF-α, tumor necrosis factor α.

versus 50.5±9.7 and 3.6±0.5 versus 6.4±0.3, respectively, $P<0.01$), whereas mannitol treatment, as a control for osmotic pressure, did not significantly affect Mmp9 mRNA or secreted protein expression. We performed the MTT assay and confirmed that high-glucose conditions did not affect cell viability (Figure 3E). To further examine the effect of high-glucose treatment on Mmp9 activity, gelatin zymography was performed. The medium from RAW264.7 cells treated with high-glucose conditions showed a decrease in gelatinolytic activity (Figure 3F), suggesting that high glucose suppresses Mmp9 activity induced by TNF-α plus $CaPO_4$ in macrophages.

Increased Nr1h2 Expression Levels by High-Glucose Treatment

To examine the mechanism by which high glucose suppresses macrophage activation, we next measured Nr1h2 mRNA expression levels. Treatment with TNF-α and $CaPO_4$ significantly decreased Nr1h2 mRNA expression compared with the control (0.2±0.04 versus 1.0±0.2, $P<0.01$) (Figure 4A), whereas high-glucose treatment significantly restored the decreased Nr1h2 mRNA expression (0.8±0.4 versus 0.2±0.04, $P<0.05$). Mannitol treatment showed no significant change in expression. As shown in Figure 4B, the same trend

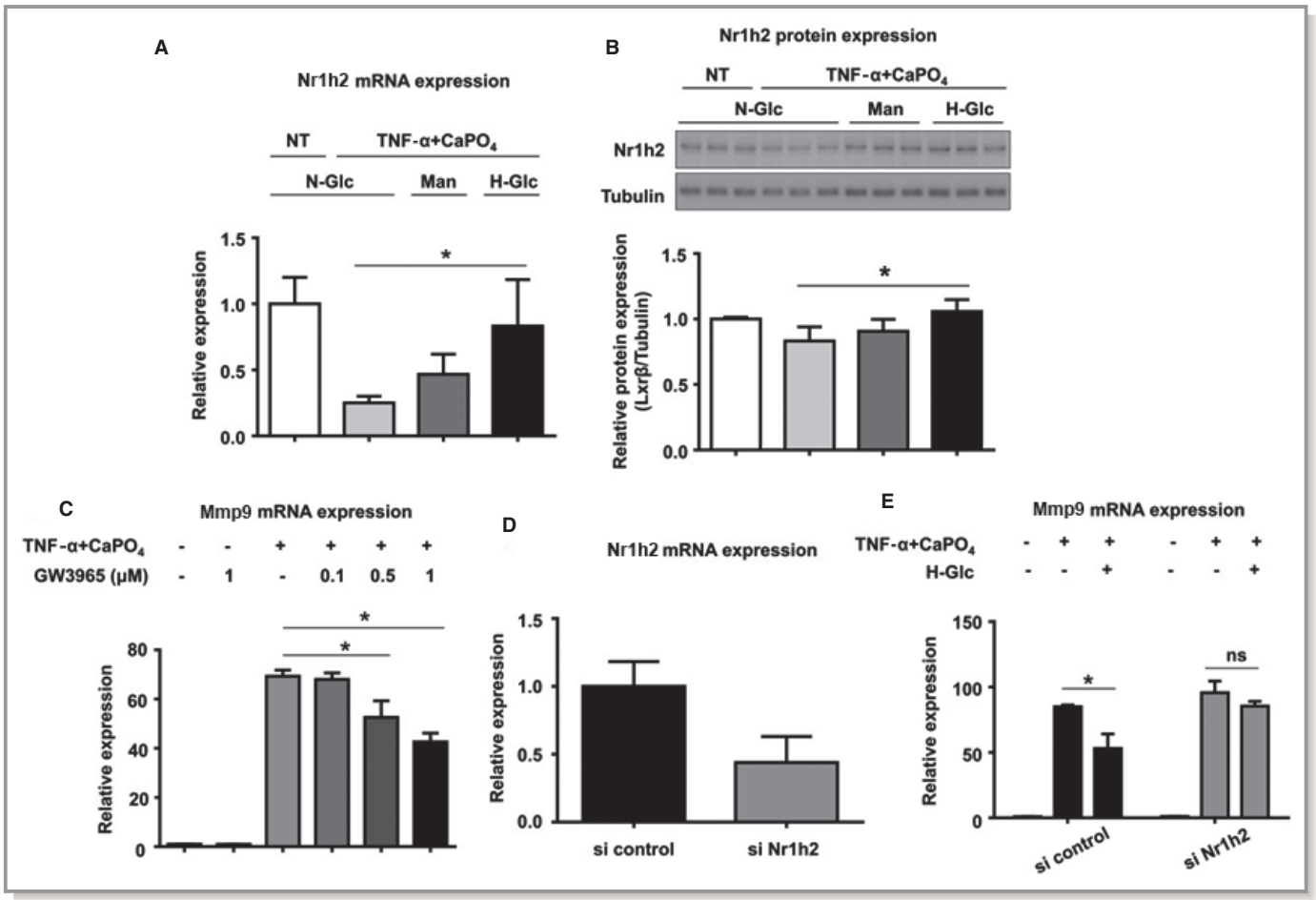

Figure 4. High-glucose treatment increased the mRNA (A) and protein (B) expression of Nr1h2. RAW264.7 cells were treated under N-Glc (5.5 mmol/L glucose) without TNF-α plus $CaPO_4$ (NT control), N-Glc with TNF-α plus $CaPO_4$, Man (5.5 mmol/L glucose and 10.5 mmol/L mannitol) and TNF-α plus $CaPO_4$, and H-Glc (15.5 mmol/L glucose) with TNF-α plus $CaPO_4$. The cells were cultured for 2 days, and Nr1h2 mRNA (A) and protein (B) expression in the cell lysates was determined by qPCR and Western blotting, respectively. C, Mmp9 mRNA expression in RAW264.7 cells under TNF-α plus $CaPO_4$ stimulation with or without GW3965, a synthetic nonsteroidal Nr1h (LXR) agonist, at 0.1 to 1 μmol/L. D, Knockdown of Nr1h2 mRNA expression by Nr1h2 siRNA. RAW264.7 cells were transfected with either a predesigned Nr1h2 siRNA or Silencer Negative Control #1. E, Mmp9 mRNA expression levels in RAW264.7 cells after transfection with siRNA. The cells were treated with control siRNA or Nr1h2 siRNA. After 4-hour transfection, 5×10^5 cells were seeded in 6-well plates. The cells were then treated with NT or TNF-α plus $CaPO_4$ under N-Glc, Man, or H-Glc for 2 days. The mRNA expression in the cell lysates was determined by qPCR. Values are presented as mean±SD for at least 3 replicates; *$P<0.05$. $CaPO_4$ indicates calcium phosphate; H-Glc, hyperglycemic conditions; LXRβ, liver X receptor β (Nr1h2); Man, normoglycemic conditions with high osmotic pressure; Mmp9, matrix metalloproteinase 9; N-Glc, normoglycemic conditions; NT, no treatment; si, small interfering; TNF-α, tumor necrosis factor α.

was observed in Nr1h2 protein expression. In the high-glucose treatment group, Nr1h2 protein expression was significantly higher than in the normal glucose treatment group, according to densitometric analysis of Western blotting (1.1±0.1 versus 0.9±0.1, $P<0.05$). Next, to examine the effect of Nr1h2 activation on macrophages, RAW264.7 cells were treated with GW3965, an Nr1h (LXR) agonist. Although GW3965 treatment did not alter Mmp9 mRNA expression in the untreated cells, it dose-dependently suppressed Mmp9 expression induced by TNF-α plus $CaPO_4$ at 0.1 to 1 μmol/L (Figure 4C). The relative expression in the cells treated with 0.5 and 1 μmol/L GW3965 was significantly lower than in the control (51.7±6.4 versus 66.7±3.1 and 40.9±3.0 versus 66.7±3.1, respectively, $P<0.05$). We also examined the effects of Nr1h2 siRNA on Mmp9 expression induced by TNF-α plus $CaPO_4$. As shown in Figure 4D, Nr1h2 siRNA knocked down Nr1h2 mRNA expression to 44% of control. In the cells treated with the siRNA control, high-glucose treatment significantly suppressed Mmp9 mRNA upregulation by TNF-α plus $CaPO_4$ (52.2±10.7 versus 86.3±2.2, $P<0.05$) (Figure 4E). In contrast, in the cells treated with Nr1h2 siRNA, the Mmp9 mRNA upregulation induced by TNF-α plus $CaPO_4$ was not suppressed by high-glucose treatment (99.3±11.2 versus 91.3±4.6). These results suggest the involvement of Nr1h2 in the mechanism by which high glucose suppresses Mmp9 expression in macrophages.

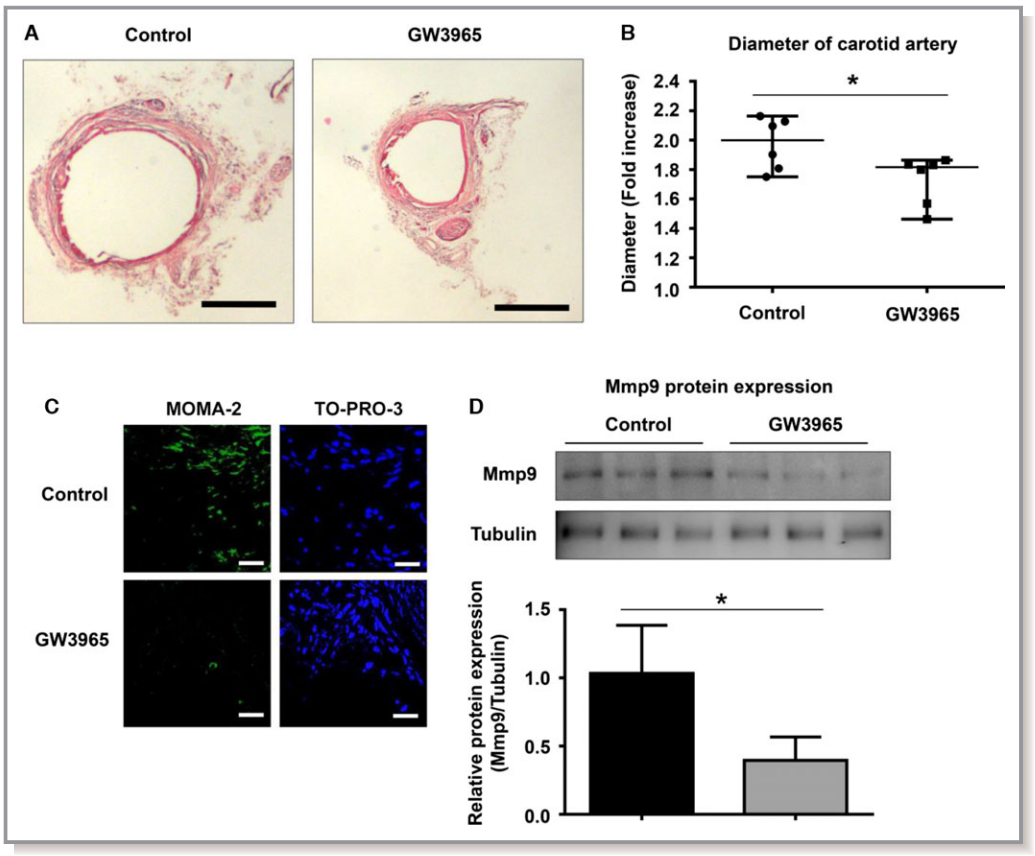

Figure 5. Nr1h (LXR) agonist suppresses $CaPO_4$-induced murine aneurysm formation. Mouse model aneurysms were created by the $CaPO_4$-induction method. The mice were divided into 2 groups: the control group (n=6) and the GW3965-administration group (n=6). GW3965 (20 mg/kg), a synthetic nonsteroidal Nr1h (LXR) agonist, or vehicle (PBS) was intraperitoneally injected into mice every day. After 2 weeks, the mice were sacrificed, and the carotid arteries were collected after perfusing with PBS. A, Representative images of mouse $CaPO_4$-induced aneurysms with hematoxylin and eosin staining are shown. Scale bar, 400 μm. B, The fold increase in arterial diameter after 2 weeks was calculated based on the maximum diameter of the artery at the time of the initial surgery and sacrifice. C, Representative immunohistochemical images for MOMA-2 and TO-PRO-3 in carotid arteries. D, Representative Western blot and densitometoric analysis of Mmp9 expression in isolated carotids. Values are presented as mean±SD for 3 replicates; *$P<0.05$. Relative expression levels for Western blotting were quantified using the ImageJ program (National Institutes of Health). $CaPO_4$ indicates calcium phosphate; LXR, liver X receptor; Mmp9, matrix metalloproteinase 9.

Inhibition of Aneurysm Formation by GW3965

Finally, we examined the effects of GW3965 on $CaPO_4$-induced aneurysm formation in mice. As shown in Figure 5A, administration of GW3965 (20 mg/kg), with the vehicle (PBS) solution as a control, was administered by intraperitoneal injection for 2 weeks, and this suppressed aneurysmal degeneration. When we calculated the fold increase based on the maximum diameter of the artery at the time of the initial surgery and sacrifice, the value for the GW3965-administration group was significantly lower than that for the control group (1.7±0.2 versus 2.0±0.2, $P<0.05$) (Figure 5B).

The number of monocytes and macrophages stained with MOMA-2 were also markedly decreased by GW3965 administration compared with the control (Figure 5C). Furthermore, GW3965 suppressed Mmp9 protein expression levels in the isolated carotids compared with the control group (0.4±0.1 versus 1.0±0.4, $P<0.05$) (Figure 5D). These results suggest that GW3965 suppresses aneurysm formation through inhibition of macrophage activation.

Discussion

MMP9 is known as a marker of classical macrophage activation and as contributing to aneurysm formation through the degradation of type IV collagen and matrix.[19–21] In the present study, we demonstrated that TNF-α plus $CaPO_4$ robustly increases Mmp9 mRNA expression and protein secretion compared with TNF-α alone in RAW264.7 cells. We previously reported that $CaPO_4$ contributes to aneurysm formation through the apoptosis of vascular smooth muscle cells with subsequent macrophage infiltration.[17] Consequently, the activation could be the result of enhanced apoptosis and an indirect positive effect of $CaPO_4$ on classical macrophage activation.

Several studies have reported that there is a reduced risk of aneurysm in DM patients,[5,11,12] and it is likely that multiple mechanisms underlie this effect. Our current study showed the inhibitory effect of type 1 and 2 DM on murine aneurysm. We suggest that the inhibitory effect is, at least in part, caused by suppression of macrophage activation because an in vitro assay using TNF-α plus $CaPO_4$ also showed an inhibitory effect of hyperglycemia on macrophage activation. Hyperglycemia, however, shows no migratory activity in RAW264.7 cells (Figure S1) and caspase-3 activity in the MOVAS mouse vascular smooth muscle cell line (Figure S2). Consequently, hyperglycemia suppresses macrophage activation without affecting migratory activity in macrophages and apoptopic activity in vascular smooth muscle cells.

To further investigate the underlying mechanisms by which hyperglycemia suppresses macrophage activation, we focused on the nuclear receptor Nr1h2, which was once categorized as an orphan receptor but later was found to act as a glucose sensor.[7] Interestingly, *Nr1h2* expression was suppressed by stimulation with TNF-α plus $CaPO_4$ under normal glucose conditions but was not affected under high-glucose conditions. Furthermore, activation of Nr1h2 by the agonist GW3965 mimicked the high-glucose effect in macrophages and suppressed Mmp9 expression and secretion. In contrast, deactivation of this receptor by siRNA canceled the suppressive effect of high glucose on Mmp9 mRNA expression and protein secretion. Together with the results showing suppression of macrophage activation and aneurysm in type 1 and 2 diabetic mice and GW3965-treated mice, these results suggest that hyperglycemia suppresses macrophage activation and aneurysm through the activation of Nr1h2.

The remaining challenges include a lack of understanding of the underlying pathway through which Nr1h2 suppresses Mmp9 expression and classical macrophage activation, as mentioned earlier. A possible pathway could be through nuclear factor κB, which is thought to play a pivotal role in TNF-α–induced inflammatory signaling. Joseph et al reported that the activation of Nr1h (LXR) decreases inducible nitric oxide synthase and cyclooxygenase 2 expression by antagonizing nuclear factor κB signaling in murine peritoneal macrophages.[22] A previous study also showed that nuclear factor κB contributes to lipopolysaccharide-induced mouse Mmp9 expression in RAW264.7 cells.[23] Consequently, further research focusing on the relationship between high glucose–induced activation of Nr1h2 and the nuclear factor κB signaling pathway as well as subsequent macrophage activation is warranted.

We used the carotid artery instead of the abdominal aorta for the mouse aneurysm model. Although another group has used the carotid artery as a model for aortic aneurysm,[24] possible physiological differences between these anatomical structures make the carotid artery an imperfect model and is a limitation of this study.

In conclusion, we showed that the inhibitory effect of DM on mouse aneurysm formation depends on suppression of macrophage activation in the arterial wall. An in vitro assay showed inhibitory effects of hyperglycemia on macrophage activation, possibly through Nr1h2 activation. Activation of Nr1h2 by GW3965 suppressed aneurysm formation in mice. Taken together, our results indicate the inhibitory effect of DM on aneurysm through the inhibition of macrophage activation by Nr1h2. Although further research is warranted to elucidate the underlying mechanisms, GW3965 could lead to a novel therapeutic approach to aneurysm.

Sources of Funding

This work was supported by the AHA project (12SDG9120024), "The role of osteoclast-like cells in abdominal aortic aneurysm formation."

Disclosures

None.

References

1. Longo GM, Xiong W, Greiner TC, Zhao Y, Fiotti N, Baxter BT. Matrix metalloproteinases 2 and 9 work in concert to produce aortic aneurysms. *J Clin Invest*. 2002;110:625–632.
2. Thompson RW, Baxter BT. MMP inhibition in abdominal aortic aneurysms. Rationale for a prospective randomized clinical trial. *Ann N Y Acad Sci*. 1999;878:159–178.
3. Domingueti CP, Dusse LM, Carvalho MD, de Sousa LP, Gomes KB, Fernandes AP. Diabetes mellitus: the linkage between oxidative stress, inflammation, hypercoagulability and vascular complications. *J Diabet Complications*. December 18, 2015; Available at: http://dx.doi.org/10.1016/j.jdiacomp.2015.12.018. Accessed March 23, 2016.
4. Tomizawa N, Nojo T, Inoh S, Nakamura S. Difference of coronary artery disease severity, extent and plaque characteristics between patients with hypertension, diabetes mellitus or dyslipidemia. *Int J Cardiovasc Imaging*. 2015;31:205–212.
5. Kent KC, Zwolak RM, Egorova NN, Riles TS, Manganaro A, Moskowitz AJ, Gelijns AC, Greco G. Analysis of risk factors for abdominal aortic aneurysm in a cohort of more than 3 million individuals. *J Vasc Surg*. 2010;52:539–548.
6. Theivacumar NS, Stephenson MA, Mistry H, Valenti D. Diabetes mellitus and aortic aneurysm rupture: a favorable association? *Vasc Endovascular Surg*. 2014;48:45–50.
7. Mitro N, Mak PA, Vargas L, Godio C, Hampton E, Molteni V, Kreusch A, Saez E. The nuclear receptor LXR is a glucose sensor. *Nature*. 2007;445:219–223.
8. Spillmann F, Van Linthout S, Miteva K, Lorenz M, Stangl V, Schultheiss HP, Tschope C. LXR agonism improves TNF-alpha-induced endothelial dysfunction in the absence of its cholesterol-modulating effects. *Atherosclerosis*. 2014;232:1–9.
9. Wang Y, Li C, Cheng K, Zhang R, Narsinh K, Li S, Li X, Qin X, Su T, Chen J, Cao F. Activation of liver X receptor improves viability of adipose-derived mesenchymal stem cells to attenuate myocardial ischemia injury through TLR4/NF-kappaB and Keap-1/Nrf-2 signaling pathways. *Antioxid Redox Signal*. 2014;21:2543–2557.
10. Robertson Remen KM, Lerner UH, Gustafsson JA, Andersson G. Activation of the liver X receptor-beta potently inhibits osteoclastogenesis from lipopolysaccharide-exposed bone marrow-derived macrophages. *J Leukoc Biol*. 2013;93:71–82.
11. Arapoglou V, Kondi-Pafiti A, Rizos D, Carvounis E, Frangou-Plemenou M, Kotsis T, Katsenis K. The influence of diabetes on degree of abdominal aortic aneurysm tissue inflammation. *Vasc Endovascular Surg*. 2010;44:454–459.
12. Miyama N, Dua MM, Yeung JJ, Schultz GM, Asagami T, Sho E, Sho M, Dalman RL. Hyperglycemia limits experimental aortic aneurysm progression. *J Vasc Surg*. 2010;52:975–983.
13. Yamanouchi D, Morgan S, Stair C, Seedial S, Lengfeld J, Kent KC, Liu B. Accelerated aneurysmal dilation associated with apoptosis and inflammation in a newly developed calcium phosphate rodent abdominal aortic aneurysm model. *J Vasc Surg*. 2012;56:455–461.
14. Kaneko H, Anzai T, Horiuchi K, Kohno T, Nagai T, Anzai A, Takahashi T, Sasaki A, Shimoda M, Maekawa Y, Shimizu H, Yoshikawa T, Okada Y, Yozu R, Fukuda K. Tumor necrosis factor-alpha converting enzyme is a key mediator of abdominal aortic aneurysm development. *Atherosclerosis*. 2011;218:470–478.
15. Ishibashi M, Sayers S, D'Armiento JM, Tall AR, Welch CL. TLR3 deficiency protects against collagen degradation and medial destruction in murine atherosclerotic plaques. *Atherosclerosis*. 2013;229:52–61.
16. Zhang HF, Zhao MG, Liang GB, Song ZQ, Li ZQ. Expression of pro-inflammatory cytokines and the risk of intracranial aneurysm. *Inflammation*. 2013;36:1195–1200.
17. Hanania R, Sun HS, Xu K, Pustylnik S, Jeganathan S, Harrison RE. Classically activated macrophages use stable microtubules for matrix metalloproteinase-9 (MMP-9) secretion. *J Biol Chem*. 2012;287:8468–8483.
18. Gong Y, Hart E, Shchurin A, Hoover-Plow J. Inflammatory macrophage migration requires MMP-9 activation by plasminogen in mice. *J Clin Invest*. 2008;118:3012–3024.
19. Sakalihasan N, Delvenne P, Nusgens BV, Limet R, Lapiere CM. Activated forms of MMP2 and MMP9 in abdominal aortic aneurysms. *J Vasc Surg*. 1996;24:127–133.
20. McMillan WD, Patterson BK, Keen RR, Pearce WH. In situ localization and quantification of seventy-two-kilodalton type IV collagenase in aneurysmal, occlusive, and normal aorta. *J Vasc Surg*. 1995;22:295–305.
21. Palombo D, Maione M, Cifiello BI, Udini M, Maggio D, Lupo M. Matrix metalloproteinases. Their role in degenerative chronic diseases of abdominal aorta. *J Cardiovasc Surg (Torino)*. 1999;40:257–260.
22. Joseph SB, Castrillo A, Laffitte BA, Mangelsdorf DJ, Tontonoz P. Reciprocal regulation of inflammation and lipid metabolism by liver X receptors. *Nat Med*. 2003;9:213–219.
23. Chou YC, Sheu JR, Chung CL, Chen CY, Lin FL, Hsu MJ, Kuo YH, Hsiao G. Nuclear-targeted inhibition of NF-kappaB on MMP-9 production by N-2-(4-bromophenyl) ethyl caffeamide in human monocytic cells. *Chem Biol Interact*. 2010;184:403–412.
24. Gallo A, Saad A, Ali R, Dardik A, Tellides G, Geirsson A. Circulating interferon-gamma-inducible Cys-X-Cys chemokine receptor 3 ligands are elevated in humans with aortic aneurysms and Cys-X-Cys chemokine receptor 3 is necessary for aneurysm formation in mice. *J Thorac Cardiovasc Surg*. 2012;143:704–710.